Selenium deficiency risk predicted to increase under future climate change

Gerrad D. Jones[a], Boris Droz[a], Peter Greve[b], Pia Gottschalk[c], Deyan Poffet[a,d], Steve P. McGrath[e], Sonia I. Seneviratne[b], Pete Smith[f], and Lenny H. E. Winkel[a,d,1]

[a]Eawag, Swiss Federal Institute of Aquatic Science and Technology, 8600 Duebendorf, Switzerland; [b]Institute for Atmospheric and Climate Science, ETH Zurich, 8092 Zurich, Switzerland; [c]Potsdam Institute for Climate Impact Research, 14473 Potsdam, Germany; [d]Institute of Biogeochemistry and Pollutant Dynamics, ETH Zurich, 8092 Zurich, Switzerland; [e]Department of Sustainable Soils and Grassland Systems, Rothamsted Research, Harpenden AL5 2JQ, United Kingdom; and [f]Institute of Biological and Environmental Sciences, School of Biological Sciences, University of Aberdeen, Aberdeen AB24 3UU, United Kingdom

Edited by Jerome Nriagu, University of Michigan, Ann Arbor, MI, and accepted by Editorial Board Member David W. Schindler January 6, 2017 (received for review July 15, 2016)

Deficiencies of micronutrients, including essential trace elements, affect up to 3 billion people worldwide. The dietary availability of trace elements is determined largely by their soil concentrations. Until now, the mechanisms governing soil concentrations have been evaluated in small-scale studies, which identify soil physicochemical properties as governing variables. However, global concentrations of trace elements and the factors controlling their distributions are virtually unknown. We used 33,241 soil data points to model recent (1980–1999) global distributions of Selenium (Se), an essential trace element that is required for humans. Worldwide, up to one in seven people have been estimated to have low dietary Se intake. Contrary to small-scale studies, soil Se concentrations were dominated by climate–soil interactions. Using moderate climate-change scenarios for 2080–2099, we predicted that changes in climate and soil organic carbon content will lead to overall decreased soil Se concentrations, particularly in agricultural areas; these decreases could increase the prevalence of Se deficiency. The importance of climate–soil interactions to Se distributions suggests that other trace elements with similar retention mechanisms will be similarly affected by climate change.

selenium | soils | global distribution | prediction | climate change

Micronutrients are essential for maintaining human health, and although they are needed in only trace amounts, deficiencies reportedly affect 3 billion people worldwide (1, 2). One such micronutrient is selenium. Inadequate dietary Se intake affects up to 1 in 7 people and is also known to affect livestock health adversely (3, 4). Because dietary Se intake depends largely on Se content in soil and bioavailability to crops (5–7), understanding the mechanisms driving soil concentrations and predicting global distributions could help prevent Se deficiency (8). However, global soil Se concentrations and the factors affecting Se distributions are largely unknown (9). Apart from soils, Se is present in all other environmental compartments [i.e., the lithosphere, hydrosphere, biosphere, and atmosphere (9)], which all play a role in global Se biogeochemical cycling and distribution (7, 10).

The factors driving soil Se concentrations [e.g., increased sorption with decreased pH and soil reduction potential (Eh) and increased clay and soil organic carbon (SOC) content; see Table S1 and refs. 7 and 11 for a review of the previously reported drivers of soil Se] have been evaluated primarily through small-scale experimentation (e.g., soil columns; see ref. 12); however, broad-scale distributions cannot be inferred from such studies. For example, soils in small-scale experiments are often manipulated [e.g., by carbon amendments (12)] to achieve desired conditions, obscuring the natural processes that may influence Se retention capacity. Additionally, climate variables, which likely affect soil Se concentrations directly as a source (e.g., deposition; see refs. 8 and 13) or indirectly by affecting soil retention of Se (e.g., sorption), are ignored in small-scale experiments. Therefore, to predict the global distributions, broad-scale analyses of soil Se drivers are essential.

Here we report on the influence of soil and climate variables on worldwide Se distributions in soils 0–30 cm deep. Our objectives were (*i*) to test hypothesized drivers of soil Se concentrations, (*ii*) to predict global soil Se concentrations quantitatively, and (*iii*) to quantify potential changes in soil Se concentrations resulting from climate change. To achieve these objectives, several regional- to continental-scale datasets reporting total soil Se concentrations [n = 33,241 data points (5, 14–29); see *SI Materials and Methods* for dataset details] and 26 environmental variables describing climate, soil physicochemical properties, irrigation, water stress, erosion, runoff, land use, soil type, lithology, bedrock depth, vegetation/canopy characteristics, and population density (30–42) (see Table S1 for details of variables) were assessed to make global predictions of soil Se concentrations for recent (1980–1999) and future (2080–2099) periods. Predictions were made using three machine-learning tools: one randomForest (RF) model and two artificial neural network models, herein referred to as "predictive models." Additionally, structural equation modeling (SEM) was used to evaluate potential mechanisms independently and to quantify complex interactions between Se and the relevant predictor variables.

Results and Discussion

After variable selection, seven variables were retained and were considered the most important factors controlling soil Se concentrations: the aridity index (AI, unitless) [i.e., the ratio of potential evapotranspiration (PET, mm/d) to precipitation (mm/d)];

Significance

The trace element selenium is essential for human health and is required in a narrow dietary concentration range. Insufficient selenium intake has been estimated to affect up to 1 billion people worldwide. Dietary selenium availability is controlled by soil–plant interactions, but the mechanisms governing its broad-scale soil distributions are largely unknown. Using data-mining techniques, we modeled recent (1980–1999) distributions and identified climate–soil interactions as main controlling factors. Furthermore, using moderate climate change projections, we predicted future (2080–2099) soil selenium losses from 58% of modeled areas (mean loss = 8.4%). Predicted losses from croplands were even higher, with 66% of croplands predicted to lose 8.7% selenium. These losses could increase the worldwide prevalence of selenium deficiency.

Author contributions: G.D.J., B.D., and L.H.E.W. designed research; G.D.J., B.D., D.P., and L.H.E.W. performed research; G.D.J., B.D., P. Greve, P. Gottschalk, S.P.M., S.I.S., P.S., and L.H.E.W. contributed data/soil samples; G.D.J., B.D., D.P., and L.H.E.W. analyzed data; and G.D.J., B.D., D.P., and L.H.E.W. wrote the paper with technical input from all authors.

The authors declare no conflict of interest.

This article is a PNAS Direct Submission. J.N. is a Guest Editor invited by the Editorial Board.

Freely available online through the PNAS open access option.

[1]To whom correspondence should be addressed. Email: lwinkel@ethz.ch.

This article contains supporting information online at www.pnas.org/lookup/suppl/doi:10.1073/pnas.1611576114/-/DCSupplemental.

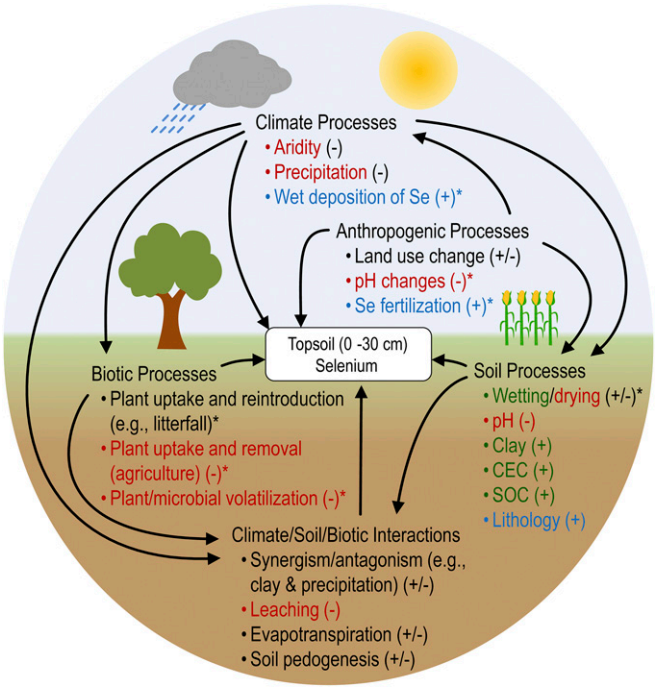

Fig. 1. Summary of the processes governing soil Se concentrations. Dominant processes (and bulleted examples) governing soil Se concentrations are indicated. Text colored in red, green, and blue indicates processes affecting soil Se losses, retention, and sources/supplies, respectively. Factors responsible for increases (+) and/or decreases (–) in soil Se as well as processes not explicitly examined in our analysis (*) are indicated.

clay content (%); evapotranspiration (ET, mm/d); lithology; pH; precipitation (mm/d); and SOC (0–30 cm depth, tons of C/ha). With these variables, the accuracy of the predictive model was high (average $R^2 = 0.67$, average cross-validation $R^2 = 0.49$, $n =$ 1,000 iterations for each model) (Fig. S1), and the precision was high [based on a low SD of the modeled prediction (0.032 mg Se/kg) relative to the mean (0.35 mg Se/kg)] (Fig. S2). For the SEM analysis, both the standardized root mean squared residual (SRMR) (0.043) and the comparative fit index (CFI) (0.962) indicated a good fit between the observed and modeled data (43). All variables retained within the SEM analysis were statistically significant (i.e., $P < 0.05$) (Fig. S3), and, based on the predictive model sensitivity analyses and the SEM regression weights, the modeling results corroborated each other strongly (see following section), suggesting that processes driving soil Se concentrations were described accurately. Because the data were averaged on a 1° scale, this modeling approach likely captures the broad-scale mechanisms but potentially misses important local-scale factors.

Soil Se concentrations were determined largely by interactions between climate and soil variables (Figs. 1 and 2, Figs. S1, S3, and S4, and Table S2). In the SEM, AI and precipitation had the greatest direct and indirect effect, respectively, on soil Se concentrations (Table S2). Based on averaged relative importance from the predictive models (Fig. S1), AI was the most important predictor (100 ± 0.3%) followed by pH (60 ± 0.7%), precipitation (58 ± 1%), ET (50 ± 0.8%), clay content (45 ± 0.4%), lithology (33 ± 0.5%), and SOC (29 ± 0.5%). Sensitivity analyses were performed on these variables to determine if the mechanisms driving soil Se concentrations changed in different zones represented by different environmental conditions (see *SI Materials and Methods* for a description). The soil Se patterns were similar between different zones, suggesting that Se drivers were consistent regardless of the environment (Fig. 2 and Fig. S4). This result suggests that the models can be used to predict soil Se concentrations in other regions of the world. In sensitivity analyses, soil Se increased with increases in clay content and with decreases in soil pH (Fig. 2 and Figs. S3 and S4), both of which are known to increase soil Se sorption (7, 44). Although soil Se is known to partition/complex with organic matter (7), soil Se was affected only weakly by changes in SOC (Figs. S1, S3, and S4 and Table S2). Furthermore, changes in lithological classes resulted in negligible changes in soil Se when other variables were held constant (Fig. S4). Although lithology was of minor importance in this study, we recognize that it can influence soil Se concentrations at local scales (45).

Climate Effects on Soil Se. Climate variables (i.e., AI, precipitation, and ET) were dominant factors driving soil Se concentrations, likely because they control leaching from soils, and observed patterns within the sensitivity and SEM analyses for all climate variables are consistent with this hypothesis. High precipitation and AI negatively affected soil Se concentrations, whereas ET positively affected soil Se concentrations (Fig. 2, Figs. S3 and S4, and Table S2). Although AI (i.e., the ratio of PET to precipitation) and precipitation are inversely related, both variables exerted negative effects on soil Se, suggesting that separate mechanisms drive these patterns. Although precipitation increases the transport of dissolved Se species in soil solution by increasing vadose zone flow, AI likely affects leaching by controlling soil redox conditions and thus Se speciation, sorption, and mobility. It has been reported that as AI increases (i.e., PET increases relative to precipitation), soils become drier (46), resulting in more oxidizing soil conditions (47). Oxidized Se species (e.g., oxyanions) are more soluble and mobile than reduced species (e.g., selenides) (7, 11, 12, 48). Therefore, soil drying likely increases the presence of oxidized/mobile soil Se species, which can be leached during subsequent rain events.

Soil drying likely increases Se mobility but also can reduce soil Se transport (although these processes likely occur at different time scales). Leaching is driven by the ratio of ET to precipitation (also known as the "evaporative index," EI) (49). As previously mentioned, precipitation increases the transport of Se through the vadose zone, but as ET increases relative to precipitation, more moisture is removed from the soil column. This removal of moisture

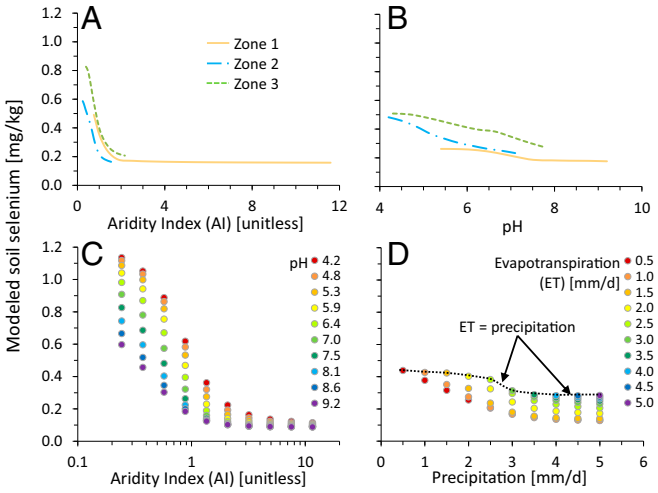

Fig. 2. Univariate and bivariate sensitivity analyses of the predictive models. (*A* and *B*) The independent effects of AI (*A*) and precipitation (*B*) were modeled by holding all other variables constant at the zonal averages as defined by the two-step clustering. (*C* and *D*) Similarly, bivariate interactions between AI and clay (*C*) and between precipitation and ET (*D*) are illustrated. These parameters were allowed to vary between the minimum and maximum observed value while all other variables were held constant at the mean value of the entire dataset ($n = 1{,}642$). The dotted line in *D* indicates the conditions in which ET = precipitation. Other bivariate interactions are presented in Fig. S3.

reduces the vadose zone flow, which in turn reduces Se mass transport. In theory, when ET and precipitation are equal, leaching should be negligible. Although ET clearly dampens the negative effects of precipitation in bivariate sensitivity analyses, a negative relationship existed between precipitation and modeled Se despite an ET:precipitation ratio of 1 (Fig. 2). This trend potentially could be explained by plant Se uptake, which has been reported to increase with ET (6). Therefore, in addition to its positive indirect effect by reducing leaching, ET also may have a direct negative effect on soil Se by increasing plant uptake. This direct negative effect was observed in the SEM analysis, but the relationship was not statistically significant and therefore was removed. Although this negative effect may exist, it appears to be less important than the role ET plays in reducing Se leaching. Given the importance of climate variables in governing soil Se concentrations, the observed patterns between AI, precipitation, ET, and modeled soil Se concentrations strongly suggest that changes in climate will result in changes in soil Se concentrations in time and space.

Climate–Soil Interactions and Soil Se. Although the direct effects of precipitation (i.e., leaching) were moderate, its indirect effects (i.e., those mediated through other variables) were approximately threefold larger (Table S2). Precipitation is known to affect soil formation (i.e., pedogenesis), and in our analyses it strongly affected AI, pH, ET, and clay content, which subsequently affect soil Se retention (Fig. S3 and Table S2). Although there was a negative direct effect between precipitation and soil Se, the sum of direct and indirect effects resulted in precipitation having a net positive effect (Table S2). Thus it is important to examine both direct and indirect effects, because interpreting only total effects can lead to erroneous conclusions about the mechanisms driving spatial patterns.

In bivariate sensitivity analyses, both synergistic and antagonistic interactions were observed and were strongest between aridity, precipitation, clay content, and pH. In univariate sensitivity analyses, when all other variables were held constant, modeled soil Se concentrations were highest under low AI (0.83 mg Se/kg), low precipitation (0.65 mg Se/kg), low pH (0.51 mg Se/kg), and relatively high clay content (0.47 mg Se/kg) (Fig. 2 and Fig. S4). It is important to note that, as long as PET is sufficiently low, environments with low precipitation can have low AI values also. Furthermore, sensitivity and SEM analyses suggest that the direct (i.e., nonmediated) effect of precipitation drives Se leaching from soils (Fig. 2 and Figs. S3 and S4), thus explaining why low values resulted in high soil Se, even though the net effect is positive (Table S2). In bivariate sensitivity analyses, soil Se concentrations exceeded these values when low AI was modeled with low pH (1.12 mg Se/kg), when low precipitation was modeled with high clay content (0.86 mg Se/kg), and when high clay content was modeled with low pH (0.56 mg Se/kg) (Fig. 2 and Fig. S3). Although Se concentrations were typically enhanced in low-AI or low-precipitation environments, both variables could suppress the effects of other variables in high-AI or high-precipitation environments (Fig. 2 and Fig. S3). These results demonstrate the dependence of soil Se concentrations on soil–climate interactions. Based on these analyses, low-Se soils are most likely to occur in arid environments and in areas with high pH and low clay content. Conversely, areas with low to moderate precipitation but relatively low aridity (e.g., cool and moist climates) and high clay content are likely to have higher soil Se concentrations.

Predicted Global Soil Se Distributions. Global predictions were made using models trained largely using temperate/midlatitude datasets (Fig. S2). Although the available data adequately described similar regions, data from tropical, extremely arid, and polar regions were almost entirely absent (to the best of our knowledge, no broad-scale soil geochemical surveys are available from these regions). As a result, predictions that were made for environments that fell outside our dataset's domain were excluded (Fig. S5). Therefore, Se predictions for 1980–1999 were retained for only 70% of land surfaces. The majority of croplands and rangelands, which are areas of primary interest, given that soil Se concentrations and bioavailability in these regions largely drive the Se status in humans and livestock, fall largely within the retained areas.

Based on predictive models, the global mean soil Se concentration for 1980–1999 was 0.322 ± 0.002 mg Se/kg (Fig. 3), similar to reported values (mean = 0.4 mg Se/kg; typical range 0.01–2 mg Se/kg) (50). Using this estimate, ~13.1 million metric tons of Se are stored in the top 30 cm of soil within the predicted area [i.e., ~70% of world's land surface (1.04×10^7 km^2); see *SI Materials and Methods* for the calculation]. Compared with other regions, predicted soil Se concentrations were generally higher (typically

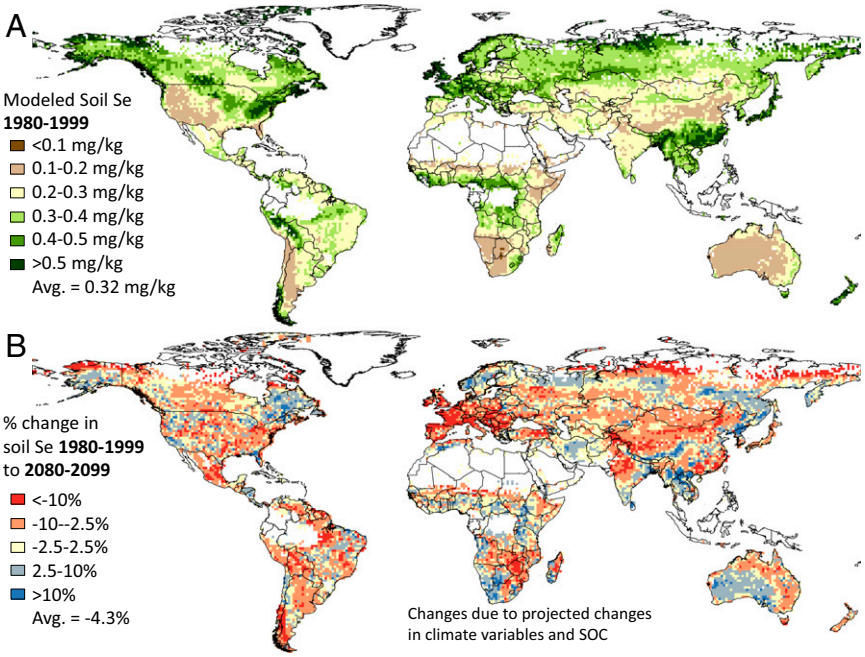

Fig. 3. Geographical representation of the predictive modeling on a 1° scale. Maps illustrate the modeled soil Se concentrations (1980–1999) (*A*) and percentage change in soil Se concentrations between recent and future (2080–2099) conditions (*B*) as a function of projected changes in climate (RCP6.0 scenario) and SOC content (ECHAM5-A1B scenario). Predictions represent the average of the predictive models and were based on the AI, soil clay content, ET, lithology, pH, precipitation, and SOC.

>0.2 mg Se/kg) (Fig. 3) in temperate and northern latitudes. In wet equatorial regions, concentrations were typically 0.3–0.5 mg Se/kg. Relatively low-Se soils (<0.2 mg Se/kg) were predicted for 15% of modeled areas and were restricted primarily to arid and semiarid regions in Argentina, Australia, Chile, China, southern Africa, and the southwestern United States. In some of these countries, low Se content in crops and livestock has been reported (3), but it is important to note that many factors contribute to low Se content in plants (e.g., plant uptake pathways, soil Se speciation, and the abundance of competing ions such as sulfate) (7).

Over- and Underpredictions of the Model. In an attempt to identify potential missing variables, we examined the residuals of the predictive models. Spatial patterns of any missing variable should match those of the residuals (Fig. S2). Overall, the models underpredicted soil Se concentrations (average residual = −0.036 ± 0.009 mg Se/kg), suggesting that Se sources may be missing from the model. On a localized level, soil Se concentrations appear to be underpredicted in regions adjacent to regions of high marine productivity (e.g., western Alaska, western Ireland, western Norway, western England, and Wales) (Fig. S2) (51). Marine environments are thought to increase soil Se concentrations via wet deposition (10, 13), and atmospheric deposition of Se thus could explain some of the model's underprediction. However, global spatial data do not exist for Se deposition and thus could not be analyzed. We included population density as a potential proxy for anthropogenic emissions, but this was one of the least important variables in the variable selection procedure. We evaluated a wide variety of qualitative factors [e.g., specific agricultural soil types (e.g., paddy soils), specific sedimentary depositional environments (e.g., glacial deposits), coal power plants, carbonaceous shale deposits, and others] that may affect soil Se distributions; however, we found no consistent discernable link between these variables and the broad-scale distribution of the model residuals.

Despite the underprediction, overall patterns of modeled soil Se distribution match the actual distribution quite closely (Fig. S2), and 71% of predicted values were within ±0.05 mg Se/kg of the observed value, indicating that a majority of the predicted data were relatively accurate. Furthermore, the sensitivity analysis and SEM trends closely match hypothesized mechanisms governing soil Se concentrations reported in the literature (Fig. 2 and Figs. S3 and S4). This finding suggests that the models are largely accurate and capture the dominant processes controlling broad-scale Se distributions. Nevertheless, future studies could include additional predictor variables, especially those that are currently unavailable, to provide better estimates of broad-scale soil Se. Furthermore, to overcome some of this study's limitations, predictions could be made on more local/regional scales using higher resolution data.

Modeled Losses of Future Soil Se. The interactions between precipitation and other soil/climate variables strongly suggest that climate changes could drive changes in soil Se concentrations. To assess the influence of changes in climate and SOC, soil Se was modeled for 2080–2099 using moderate climate change scenarios [Representative Concentration Pathways (RCP) 6.0 for precipitation, AI, and ET (52) and European Centre/Hamburg Model (ECHAM) 5-A1B for SOC (33)]. Other climate scenarios (e.g., RCP 8.5) were not used because SOC data were available only for A1B scenarios, which are most similar to RCP 6.0.

Future predictions were made for the entire globe, but, based on the filtering criteria used (*SI Materials and Methods*), predictions were retained for ∼48% of the global land area. Based on these pixels alone, soil Se concentrations were predicted to drop by 4.3% on average, from 0.331 ± 0.003 mg Se/kg in 1980–1999 to 0.316 ± 0.002 mg Se/kg in 2080–2099, as a result of changes in climate and SOC concentrations (Fig. 3). For soil at a depth of 0–30 cm, this loss corresponds to ∼403,763 tons of Se over 100 y, or 4,037.6 tons of Se lost per year (see *SI Materials and Methods* for the calculation), an amount that is ∼20–30% of the total estimated Se mass that is cycled yearly through the troposphere [i.e., 13,000–19,000 tons (assumed to be metric tons)/y (10)], although our estimate is only for 48% of the land surface. Our modeling approach is not a mass balance model, so Se fate could not be investigated. Nonetheless, changes in Se concentrations in other environmental compartments are known from the past. For example, marine Se concentrations throughout various periods of the Phanerozoic eon have been 1.5–2 orders of magnitude lower than current oceanic concentrations (53).

Based on areas with future predictions (7.19×10^7 km^2), 58% of lands were predicted to lose soil Se (i.e., ΔSe less than −2.5%; mean change = −8.4%); 20% were predicted to undergo minor changes (i.e., −2.5% < ΔSe < 2.5%; mean change = −0.3%); and 22% were predicted to gain soil Se (i.e., ΔSe > 2.5%; mean change = 5.7%) as a result of changes in climate and SOC (Fig. 3). Predicted soil Se losses were driven largely by changes in AI, whereas soil Se gains were driven largely by changes in precipitation and SOC (Fig. S1). Compared with the total land surface, croplands were expected to lose more soil Se. Based on future predictions for croplands (7.55×10^6 km^2), 66% of lands were predicted to lose soil Se (ΔSe less than −2.5%; mean change = −8.7%); 15% were predicted to undergo minor changes (−2.5% < ΔSe < 2.5%; mean change = −0.4%); and 19% were predicted to gain soil Se (ΔSe > 2.5%; mean change = 7.3%) (Fig. 3 and Fig. S6). Global pasture lands also were predicted to lose soil Se, but to a lesser extent than croplands, suggesting that Se deficiency in livestock could increase. Based on future predictions for pasture lands (2.55×10^7 km^2), 61% of lands were predicted to lose soil Se (ΔSe less than −2.5%; mean change = −8.0%); 19% were predicted to undergo minor changes (−2.5% < ΔSe < 2.5%; mean change = −0.4%); and 21% were predicted to gain soil Se (ΔSe > 2.5% mean change = 8.2%) (Fig. 3 and Fig. S6). Areas with notable losses (i.e., ΔSe less than −10%) include croplands of Europe and India, pastures of China, Southern Africa, and southern South America, and the southwestern United States (Fig. 3 and Fig. S6). Areas of notable gain (ΔSe > 10%) are scattered across Australia, China, India, and Africa (Fig. 3 and Fig. S6).

Temporal Changes in Soil Se. Although our analysis indicates that future climate change will likely result in widespread changes in soil Se, it does not indicate rates of change. To understand the temporal changes in soil Se concentrations better, we analyzed for soil Se and SOC in a subset of agricultural samples collected from the Broadbalk Experiment (Rothamsted, United Kingdom) between 1865 and 2010. Soil samples were taken from a control plot (unfertilized since 1843) and two "wilderness" plots (a maintained grassland and woodland), which were converted from the control plot in 1882 (*SI Materials and Methods*, and Table S3). The accumulation of Se in soil through time was statistically greater in the wilderness plots than in the control plot [one-way analysis of covariance (ANCOVA); year: $F(1, 31) = 20.7$, $P < 0.01$; plot $F(2, 31) = 17.3$, $P < 0.01$]. When controlling for SOC, however, there were no statistical differences between the plots (ANCOVA; SOC: $F(1, 30) = 10.7$, $P < 0.01$; year: $F(1, 30) = 6.0$, $P < 0.05$; plot: $F(2, 30) = 3.2$, $P > 0.05$), indicating that increases in SOC were driving soil Se accumulation in the model (Fig. S7), as is consistent with the results of the future modeling (Fig. S1). Natural changes in soil Se concentrations previously have been hypothesized to occur over longer time scales (e.g., hundreds to thousands of years) (54); however, given that SOC and Se began to accumulate on these plots immediately after conversion, these results suggest that changes in soil Se will follow environmental changes rapidly, perhaps on an annual to decadal time scale. Between ∼1880 and 1980, soil Se concentrations increased by ∼15, 35, and 60% on the control, grassland, and woodland plots, respectively (Fig. S7), indicating that the magnitude of changes predicted to occur by the end of the 21st century is plausible. The rates of change in soil Se concentrations

following environmental perturbations is largely unstudied and should be evaluated further to understand soil Se dynamics better.

Outlook

One of our aims was to identify the broad-scale mechanisms governing soil Se retention. Therefore, at a 1° resolution, the data used are likely too coarse to evaluate or identify the influence of many small- to regional-scale factors (e.g., local sources, specific soil and rock types, and so forth) affecting soil Se retention. To evaluate small-scale soil Se distributions or to test locally relevant hypotheses, scale-appropriate models are necessary.

Although some effects of climate change on global food security are predictable (e.g., decreased food production resulting from increased water stress), the predicted widespread reductions in soil Se caused by climate change were less foreseeable. Changes in other factors (e.g., specific Se sources, soil properties, soil and rock weathering, and others.) will likely have an additional effect on soil Se, but these factors were not analyzed because future projections for soil pH and clay content and spatial information on the contributions of anthropogenic and natural sources of Se are currently unavailable. These variables are likely to have an effect on soil Se concentrations. For example, given changes in industrial SO_x and NO_x emissions (55), soil pH will likely increase (56). Increases in pH may result in further losses of soil Se concentrations, given that soil Se and soil pH are inversely related. Therefore, updated soil Se predictions are likely to change as additional data become available.

Given the importance of climate–soil interactions on soil Se distributions, it is likely that other trace elements with similar retention mechanisms will experience similar reductions as the result of climatic change. Coupled with micronutrient stripping from agricultural lands (57), predicted losses of total Se in soils indicate that the nutritional quality of food may decrease, thereby increasing the worldwide risk of micronutrient deficiency. However, as stated previously, total soil Se concentrations are not the only factor determining Se levels in plants. Lower Se levels in soils could potentially compound the problems associated with the decrease in the nutritional value of some plants resulting from elevated atmospheric CO_2 concentrations (58). Potential micronutrient losses from agricultural soils could be offset by implementing agricultural practices that increase their retention [e.g., organic carbon (OC) adjustment]; however, such strategies may not increase soil Se in areas of increasing aridity, given the importance of AI in governing soil Se concentrations. Where soils cannot be manipulated to increase the long-term retention of Se, broad-scale micronutrient fertilization may be necessary to maintain an adequate nutrient content in crops.

Materials and Methods

Total Se concentrations in soils (mg Se/kg soil, reported herein as mg Se/kg; soils were air dried or oven dried) 0–30 cm deep (n = 33,241 samples) were obtained from Brazil, Canada, China, Europe, Japan, Kenya, Malawi, New Zealand, South Africa, and the United States (see *SI Materials and Methods* for dataset details and a discussion about which Se datasets were used, Fig. S8). Samples derived from stream sediments were excluded from this analysis. In addition, we obtained 26 variables describing factors hypothesized to control soil Se concentrations and moderate climate change projections (RCP 6.0 for climate and A1B for SOC data; see Table S1 for variable descriptions and citations). All data within a 1° cell were averaged and represented by a single value. To minimize the influence of errors and/or outliers within the datasets, pixels containing fewer than five Se data points were removed from the analysis (*SI Materials and Methods*). The final soil Se dataset consisted of n = 1,642 aggregated points. Four techniques for selecting variables [e.g., correlations, principal components analysis (PCA), backward elimination modeling, and RF node purity analyses; see *SI Materials and Methods*] were used to retain the following variables for predictive analysis: AI, clay content, ET, lithology, pH, precipitation, and SOC at a soil depth of 0–30 cm. Although 16 lithological classes were present within the raster dataset, classes that were represented by too few soil Se data points (n < 200) were grouped together instead of being deleted (Fig. S4 and see *SI Materials and Methods* for further discussion).

Predictive modeling was performed using three machine-learning models (one RF and two artificial neural network models) (*SI Materials and Methods*). Each model was iterated 1,000 times using 90% of the data for model training and 10% of the data for cross-validation for each iteration. The training and cross-validation data were chosen at random for each iteration. The model predictions were averaged to estimate recent (1980–1999) global soil Se concentrations; however, predictions were considered valid only if the environmental parameters for each pixel fit within the domain of the observed data (Fig. S5).

Sensitivity analyses were performed during each iteration to investigate the independent effect of each variable on modeled soil Se concentrations. Based on all input variables, three environmental zones were identified using a two-step cluster analysis (*SI Materials and Methods*). Based on the data from each zone, individual parameters were allowed to vary while all other variables were held constant at the zonal averages. By using different zones, we could model the response of soil Se to changes in particular variables under different environmental conditions. These analyses allowed us to identify the most likely mechanism driving soil Se concentrations by comparing the predictions made by various hypotheses (Table S1) with the patterns observed in the sensitivity analysis.

Each predictive model was also used to predict future (2080–2099) soil Se concentrations based on projected climate and SOC changes. Future datasets did not exist for all variables (e.g., clay content); such variables were included within the prediction, but their values were identical in the two time points. Although some variables (e.g., sand, silt, and clay content) are not likely to change considerably, changes in other variables, such as soil pH, are likely to result in changes in soil Se concentrations. Therefore, we discuss only potential changes in soil Se concentrations resulting from climate change instead of reporting actual soil Se concentrations. Future predictions were retained if the SD of the future prediction was <10% of the mean prediction (i.e., SD < 0.1*mean) or if the three models predicted the same direction (loss or gain) of change (*SI Materials and Methods*). Only pixels that overlapped between the 1980–1999 and 2080–2099 time periods (~48% of the global land surface) were reported in discussions of future changes.

In addition to predictive analyses, we developed a conceptual model describing broad-scale soil Se concentrations based on mechanistic knowledge gained from the literature and on climate knowledge gained from predictive analyses. This proposed model was evaluated using SEM (*i*) to test different hypotheses proposed to govern soil Se concentrations, (*ii*) to evaluate simultaneously the relative importance of these different hypothesized mechanisms, and (*iii*) to evaluate the direct and indirect effects (i.e., mediated effects) of the variables on soil Se concentrations (the direct effects generated from the SEM analysis are analogous to the univariate sensitivity analysis of the machine-learning models). Although SEM is not predictive, it has advantages over the predictive models because it can quantify both the direct and indirect effects of all variables more easily, and it was used to help identify important interactions among variables. The SEM was considered a good fit if the SRMR was ≤0.8 and the CFI was ≥0.95 (43). Only statistically significant (α = 0.05) variables were retained in the SEM analysis. All error intervals presented represent 95% confidence intervals unless otherwise noted. All statistical procedures were performed using the software packages R (v. 3.3.2, R Development Core Team, Vienna), SPSS (v. 22, IBM. Corp., Armonk, NY), and SPSS-Amos (v. 22, IBM Corp., Armonk, NY), and all spatial procedures were performed using the software packages ArcMap [v. 10.2.2, Environmental Systems Research Institute (ESRI), Redlands, CA] and R.

ACKNOWLEDGMENTS. We thank S. Adcock, M. Broadley, E. C. da Silva, Jr., A. Chilimba, K. Dhillon, A. Donald, A. Eqani, L. Guilherme, E. Joy, K. Macey, A. Meharg, P. Morris, G. Paterson, H. Shen, J. van Ryssen, J. Wilford, and J. Yanai for providing data; T. Blazina for digitizing the Chinese soil Se data; J. Hernandez for helping us obtain samples from the Rothamsted archive; M. Glendining for providing data for the Broadbalk soil experiment; K. Abbaspour, K. Coleman, C. F. Randin, H. F. Satizábal, and R. Siber for input on methodological approaches; C. Stengel for assistance in analyzing soil samples for Se; R. Jones for comments on an earlier draft of this paper; U. Beyerle and J. Sedlacek for processing the Climate Model Intercomparison Project (CMIP) Phase 5 data; the World Climate Research Programme's Working Group on Coupled Modeling, which is responsible for CMIP; and the climate modeling groups for producing and making available their model output. The US Department of Energy's Program for Climate Model Diagnosis and Intercomparison provides coordinating support for CMIP and led the development of software infrastructure in partnership with the Global Organization for Earth System Science Portals. This work was supported by Swiss National Science Foundation Grants PP00P2_133619 and PP00P2_163747 and Eawag, the Swiss Federal Institute of Aquatic Science and Technology. P.S. is supported by the Delivering Food Security on Limited Land (DEVIL) project (UK Natural Environmental Research Council NE/M021327/1) funded by the Belmont Forum/Joint Programming Initiative on Agriculture, Food Security and Climate Change (FACCE-JPI) and by UK Biotechnology and Biological Sciences Research Council Project BB/L000113/1. Rothamsted Research is grant-aided by the UK Biotechnology and Biological Sciences Research Council.

1. Stoltzfus RJ, Mullany L, Black RE (2004) *Iron Deficiency Anaemia. Comparative Quantification of Health Risks: Global and Regional Burden of Disease Attribution to Selected Major Risk Factors*, eds Ezzati M, Lopez AD, Rodgers A, Murray CJL (World Health Organization, Geneva), Vol 1, pp 163–210.
2. Adamson P (2004) *Vitamin and Mineral Deficiency: A Global Progress Report* (Micronutrient Initiative, UNICEF, Ottawa).
3. Fordyce FM (2013) Selenium deficiency and toxicity in the environment. *Essentials of Medical Geology*, eds Selinus O, et al. (Springer, London), pp 373–415.
4. James L, et al. (1989) *Selenium Poisoning in Livestock: A Review and Progress. Selenium in Agriculture and the Environment* (Soil Science Society of America and American Society of Agronomy, Madison, WI), pp 123–131.
5. Chilimba ADC, et al. (2011) Maize grain and soil surveys reveal suboptimal dietary selenium intake is widespread in Malawi. *Sci Rep* 1(72):72.
6. Renkema H, et al. (2012) The effect of transpiration on selenium uptake and mobility in durum wheat and spring canola. *Plant Soil* 354(1-2):239–250.
7. Winkel LHE, et al. (2015) Selenium cycling across soil-plant-atmosphere interfaces: A critical review. *Nutrients* 7(6):4199–4239.
8. Sun G-X, et al. (2016) Distribution of soil selenium in China is potentially controlled bydeposition and volatilization? *Sci Rep* 6:20953.
9. Winkel LHE, et al. (2012) Environmental selenium research: From microscopic processes to global understanding. *Environ Sci Technol* 46(2):571–579.
10. Wen H, Carignan J (2007) Reviews on atmospheric selenium: Emissions, speciation and fate. *Atmos Environ* 41(34):7151–7165.
11. Fernández-Martínez A, Charlet L (2009) Selenium environmental cycling and bioavailability: A structural chemist point of view. *Rev Environ Sci Biotechnol* 8(1):81–110.
12. Neal RH, Sposito G (1991) Selenium mobility in irrigated soil columns as affected by organic carbon amendment. *J Environ Qual* 20(4):808–814.
13. Blazina T, et al. (2014) Terrestrial selenium distribution in China is potentially linked to monsoonal climate. *Nat Commun* 5(4717):4717.
14. Lee GK, et al. (2016) *The Geochemical Atlas of Alaska, 2016*, US Geologic Survey Data Series 908, p. 25, GIS database available at https://pubs.er.usgs.gov/publication/ds908. Accessed January 28, 2017.
15. Fichtner SS, et al. (2007) Estudo da composição mineral de solos, forragens e tecido animal de bovinos do município De Rio Verde, Goiás: Cobre, molibdênio e selênio. *Pesqui Agropecu Trop* 20(1):1–6.
16. Faria L (2009) Levantamento Sobre Selênio em Solos e Plantas do Brasil e sua Aplicação em Plantas Forrageiras. Thesis (Universidade De São Paulo, São Paulo, Brasil).
17. Gabos MB, Alleoni LRF, Abreu CA (2014) Background levels of selenium in some selected Brazilian tropical soils. *J Geochem Explor* 145:35–39.
18. Carvalho GS (2011) Selênio e Mercúrio em Solos sob Cerrado Nativo. Thesis (Universidade Federal de Lavras, Lavras, Brazil).
19. Smith DB, et al. (2005) Major- and Trace-Element Concentrations in Soils from Two Continental-Scale Transects of the United States and Canada, US Geologic Survey Open-File Report 2005-1253. Available at https://pubs.usgs.gov/of/2005/1253/pdf/OFR1253.pdf. Accessed January 28, 2017.
20. Friske P, et al. (2014) Soil Geochemical, Mineralogical, Radon and Gamma Ray Spectrometric Data from the 2007 North American Soil Geochemical Landscapes Project in New Brunswick, Nova Scotia, and Prince Edward Island; Geological Survey of 446 Canada, Open File 6433 (revised). Available at http://geogratis.gc.ca/api/en/nrcan-rncan/ess-sst/fa531017-b8bf-50c0-b7e4-a7764361415b.html. Accessed January 28, 2017.
21. Friske P, et al. (2013) Soil Geochemical, Radon and Gamma Ray Spectrometric Data from the 2008 and 2009 North American Soil Geochemical Landscapes Project Field Surveys, Open File 7334. Available at http://geoscan.nrcan.gc.ca/starweb/geoscan/servlet.starweb?path=geoscan/fullf.web&search1=R=292514. Accessed January 28, 2017.
22. Rawlins B, et al. (2012) The Advanced Soil Geochemical Atlas of England and Wales. (British Geological Survey, Keyworth, UK).
23. Reimann C, et al. (2014) Distribution of elements/parameters in agricultural and grazing land soil in Europe. *Chemistry of Europe's Agricultural Soils. Part A: Methodology and Interpretation of the GEMAS Data Set*, eds Reimann C, Birke M, Demetriades A, Filzmoser P, O'Connor P (Bundesanstalt für Geowissenschaften und Rohstoffe, Hannover, Germany), pp 103–474.
24. Yamada H, Kamada A, Usuki M, Yanai J (2009) Total selenium content of agricultural soils in Japan. *Soil Sci Plant Nutr* 55(5):616–622.
25. Maskall JE, Thornton I (1989) The mineral status of Lake Nakuru National Park, Kenya - a reconnaissance survey. *Afr J Ecol* 27(3):191–200.
26. Joy EJM, et al. (2015) Soil type influences crop mineral composition in Malawi. *Sci Total Environ* 505:587–595.
27. Martin A, et al. (2016) The regional geochemical baseline soil survey of southern New Zealand: Design and initial interpretation. *J Geochem Explor* 167:70–82.
28. Zheng C (1994) *Atlas of Soil Environmental Background Value in the People's Republic of China* (China Environmental Science Press, Beijing), p 195.
29. ARC-ISCW (2005) Overview of the Agricultural Natural Resources of South Africa: Report No. GW/A/2004/13. (ARC-Institute for Soil, Climate and Water, Pretoria, South Africa).
30. Greve P, Seneviratne SI (2015) Assessment of future changes in water availability and aridity. *Geophys Res Lett* 42(13):5493–5499.
31. Stackhouse PW, Jr, et al. (2006) Fast longwave and shortwave radiative flux (FLASHFlux) products from CERES and MODIS measurements. *Proceedings of the 12th Conference on Atmospheric Radiation*, July 10–14, Madison, WI, (American Meteorological Society, Boston), pp 1–6.
32. Hengl T, et al. (2014) SoilGrids1km–global soil information based on automated mapping. *PLoS One* 9(8):e105992.
33. Gottschalk P, et al. (2012) How will organic carbon stocks in mineral soils evolve under future climate? Global projections using RothC for a range of climate change scenarios. *Biogeosciences* 9(8):3151–3171.
34. Trabucco A, Zomer R (2010) Global soil water balance geospatial database. CGIAR Consortium for Spatial Information. Published online, available from the CGIAR-CSI GeoPortal at www.cgiar-csi.org. Accessed January 28, 2017.
35. Siebert S, Henrich V, Frenken K, Burke J (2013) *Update of the digital global map of irrigation areas to version 5* (Rheinische Friedrich-Wilhelms-Universität, Bonn, Germany and Food and Agriculture Organization of the United Nations, Rome, Italy).
36. Milly PC, Dunne KA, Vecchia AV (2005) Global pattern of trends in streamflow and water availability in a changing climate. *Nature* 438(7066):347–350.
37. Nachtergaele F, et al. (2010) Global land degradation information system (GLADIS), Beta version. (Food and Agriculture Organization of the United Nations, Rome), Technical Report 17.
38. Hartmann J, Moosdorf N (2012) The new global lithological map database GLiM: A representation of rock properties at the Earth surface. *Geochem Geophys Geosyst* 13(12):1–37.
39. Hollmann R, et al. (2013) The ESA climate change initiative: Satellite data records for essential climate variables. *Bull Am Meteorol Soc* 94(10):1541–1552.
40. Broxton PD, Zeng XB, Sulla-Menashe D, Troch PA (2014) A global land cover climatology using MODIS data. *J Appl Meteorol Climatol* 53(6):1593–1605.
41. Lefsky MA (2010) A global forest canopy height map from the Moderate Resolution Imaging Spectroradiometer and the Geoscience Laser Altimeter System. *Geophys Res Lett* 37(15):L15401.
42. Center for International Earth Science Information Network - CIESIN – Columbia University (2016) Documentation for the Gridded Population of the World, Version 4 (GPWv4). (NASA Socioeconomic Data and Applications Center, Palisades NY) Available at sedac.ciesin.columbia.edu/data/collection/gpw-v4/documentation. Accessed January 28, 2017.
43. Hu L, Bentler PM (1999) Cutoff criteria for fit indexes in covariance structure analysis: Conventional criteria versus new alternatives. *Struct Equ Modeling* 6(1):1–55.
44. Rovira M, et al. (2008) Sorption of selenium(IV) and selenium(VI) onto natural iron oxides: Goethite and hematite. *J Hazard Mater* 150(2):279–284.
45. Dhillon KS, Dhillon SK (2014) Development and mapping of seleniferous soils in northwestern India. *Chemosphere* 99:56–63.
46. Western AW, Grayson RB, Blöschl G (2002) Scaling of soil moisture: A hydrologic perspective. *Annu Rev Earth Planet Sci* 30(1):149–180.
47. Silver WL, Lugo A, Keller M (1999) Soil oxygen availability and biogeochemistry along rainfall and topographic gradients in upland wet tropical forest soils. *Biogeochemistry* 44(3):301–328.
48. Guo L, Frankenberger WT, Jury WA (1999) Evaluation of simultaneous reduction and transport of selenium in saturated soil columns. *Water Resour Res* 35(3):663–669.
49. Boulding JR, Ginn JS (2003) *Practical Handbook of Soil, Vadose Zone, and Ground-Water Contamination: Assessment, Prevention, and Remediation* (CRC, Boca Raton, FL).
50. Fordyce F (2007) Selenium geochemistry and health. *Ambio* 36(1):94–97.
51. Ocean Biology Processing Group (2003) *MODIS Aqua Level 3 Global Monthly Mapped 4 km Chlorophyll a. Ver. 6.* (Physical Oceanography Distributed Active Archive Center, Pasadena, CA).
52. Taylor KE, Stouffer RJ, Meehl GA (2012) An overview of Cmip5 and the experiment design. *Bull Am Meteorol Soc* 93(4):485–498.
53. Long JA, et al. (2015) Severe selenium depletion in the Phanerozoic oceans as a factor in three global mass extinction events. *Gondwana Res* 36:209–218.
54. Yu T, et al. (2014) The origin and geochemical cycle of soil selenium in a Se-rich area of China. *J Geochem Explor* 139:97–108.
55. Intergovernmental Panel on Climate Change (2014) *Climate Change 2014: Synthesis Report*, eds IPCC Core Writing Team, Pachauri RK, Meyer LA (IPCC, Geneva).
56. Kirk GJD, Bellamy PH, Lark RM (2010) Changes in soil pH across England and Wales in response to decreased acid deposition. *Glob Change Biol* 16(11):3111–3119.
57. Jones DL, et al. (2013) Review: Nutrient stripping: The global disparity between food security and soil nutrient stocks. *J Appl Ecol* 50(4):851–862.
58. Myers SS, et al. (2014) Increasing CO_2 threatens human nutrition. *Nature* 510(7503):139–142.
59. Oldfield J (2002) *Selenium World Atlas*. (Selenium-Tellurium Development Association, Grimbergen, Belgium). Updated edition.
60. Satizábal MH, Pérez-Uribe A (2007) Relevance metrics to reduce input dimensions in artificial neural networks. *Proceedings of the 17th International Conference on Artificial Neural Networks, September 9–13*, eds Sá JMd, Alexandre L, Duch W, Mandic D (Springer, Berlin), pp 39-48.
61. Carpita M, Sandri M, Simonetto A, Zuccolotto P (2013) Football mining with R. *Data Mining Applications with R*, eds Zhao Y, Cen Y (Academic, Waltham, MA), pp 397–433.
62. Nocedal J, Wright S (2006) *Numerical Optimization* (Springer Science & Business Media, New York), 2nd Ed.
63. Knights JS, Zhao FJ, Spiro B, McGrath SP (2000) Long-term effects of land use and fertilizer treatments on sulfur cycling. *J Environ Qual* 29(6):1867–1874.
64. Hewitt A, Reynolds C (1990) Dissolution of metals from soils and sediments with a microwave-nitric acid digestion technique. *Spectrosc.* 11(5):187–192.
65. Binstock DA, et al. (1990) Validation of Methods for Determining Elements in Solid Waste by Microwave Digestion. *Waste Testing and Quality Assurance*, ed Friedman D (ASTM International, Philadelphia), Vol 2, pp 259–270.
66. Ramankutty N, Evan AT, Monfreda C, Foley JA (2008) Farming the planet: 1. Geographic distribution of global agricultural lands in the year 2000. *Global Biogeochem Cycles* 22(1):GB1003.